Hindawi
Journal of Advanced Transportation
Volume 2018, Article ID 4182927, 11 pages
https://doi.org/10.1155/2018/4182927

Research Article

Cognitive Waveform Design for Radar-Communication Transceiver Networks

Yu Yao [1] **and Lenan Wu** [2]

[1] *School of Information Engineering, East China Jiaotong University, Nanchang 330031, China*
[2] *School of Information Science and Engineering, Southeast University, Nanjing 210096, China*

Correspondence should be addressed to Yu Yao; 1057604987@qq.com

Received 4 December 2017; Revised 1 March 2018; Accepted 20 March 2018; Published 24 April 2018

Academic Editor: Nandana Rajatheva

The system architecture for cognitive radar-communication (CRC) transceiver is proposed. A cognitive waveforms design approach, which is suitable for simultaneously performing both data communication and target detection, is presented. This approach aims at estimating target scattering coefficient (TSC) from the radar scene and facilitating high data rate communications. In order to minimize the mean square error (MSE) of the TSC, a convex cost function is established. The peak to average power ratio- (PAPR-) constrained optimal solution is achieved by applying the Kalman filtering-based strategy to design the set of ultra-wideband (UWB) transmission pulses and embed into them the information data with the M-ary position phase shift keying modulation technique. In addition to theoretical considerations, the simulation results show an improvement in target scattering coefficient (TSC) estimation and target detection probability as the number of iterations increases, while still transmitting data rates in the range of several Mbps with low bit error rates between CRC transceivers.

1. Introduction

The integration of multiple functions such as radar tasks and communication applications has attracted substantial interest in recent years and sparked a number of research initiatives [1–4]. It is studied in [5] that the intelligent transportation system (ITS) employs communications device to convey traffic information and utilizes the radar device to sense the traffic circumstance. The demand of ITS is the motive to develop radar-communication integration system.

1.1. Background. The objective of the joint design is to increase both energy efficiency and spectrum efficiency and to reduce manufacturing cost. The design of integrated waveform can be classified into two main categories. One is based on the multiplexing technique including space division multiplexing (SDM) [6], time division multiplexing (TDM) [7], and frequency division multiplexing (FDM) [8], and code division multiplexing (CDM) [9]. However, such a class has the same drawback that radar and communication cannot operate in some domain, simultaneously. For instance, the radar and communication cannot operate at the same time slot for the methods based on the TDM technique. The other is based on waveform sharing and has two types. One is that the communication information is hidden in the conventional radar waveforms [10]; the other is that the communication waveforms generally employed are either slightly changed or not [11].

The conventional orthogonal frequency division multiplexing (OFDM) waveform in communication is continuous in general [12–14]. In contrast, it is noncontinuous for pulse radar. Moreover, most of the employed OFDM waveforms in radar consist of OFDM pulse train which is indispensable for communication, and one pulse only contains one OFDM symbol. If the integrated radar and communication system employs the continuous OFDM waveform, the transmit and receive antennas need to be well separated, which is difficult to realize in practice, especially in those cases when either transmit or receive antennas are close to each other. If the integrated OFDM waveform is impulse, the transmit and receive antennas can be shared and the number of antennas will be reduced to half. Furthermore, the problem of isolation

between transmit and receive antennas can be perfectly settled. For the communication applications, however, the data rate will decrease because the radar duty ratio is 10% in some cases; that is, the operation time of communication becomes 10% of what it was.

These works have adopted OFDM techniques fused with ultra-wideband (UWB) technologies to realize the communication-radar integration. However, these designs create other implementation issues, such as excessive demand of signal processing power, high-speed analog-to-digital circuitry, and agile radio frequency front end for multimode operation. Furthermore, systems employing UWB-OFDM for localization [13, 14] utilize the same waveform family for designing joint communication-radar signals. Consequently, these methods share a common drawback due to the fact that the autocorrelation of UWB-OFDM signals depend on both the location of the notch and the OFDM signal bandwidth. Hence, although the radar target range estimation is unaffected by the presence of an OFDM signal, its range resolution depends on the notch bandwidth into which the OFDM signal is embedded. Literature [15] presents the system employing UWB pulse position modulation (PPM) for designing joint communication-radar signals. Compared to the conventional OFDM system, the system bit error rate (BER) performance is poor relatively [16, 17].

Cognitive radar (CR) system can adjust its transmit waveform and receive filter adaptively based on the prior knowledge of targets and the environment and thus has great potential in enhancing the detection and recognition performance for extended targets [18]. In CR [19], cognition plays a critical role in the feedback loop, which includes long-term memory, for example, geographic map and elevation model, and short-term memory developed by the receiver online. By using prior information, the work mode, transmit waveform, and signal processing approach of CR can be optimized to yield better performance.

The wideband cognitive radar is not sensitive to active and passive interference [20]. It is very important in intelligent transmitting. In the wideband cognitive radar system, the extended target has a complex target impulse response (TIR) [21], which is the target scattering coefficient (TSC) in the frequency domain [22]. The estimation of TSC has gotten lots of attention in the recent research of radar system [23–25]. Literature [23] models the extended target as TIR function unchanged in the waveform design. Reference [26] models the extended target as a wide sense stationary-uncorrelated scattering TIR model, considering the change of target view angle and the strong correlation of TSC during the pluses interval. The interference might be comprised of clutter and noise. Clutter, such as unwanted ground returns and environment clutter, is assumed to be signal dependent and noise is signal independent too [27]. The radar reflection characteristics of the surrounding environment are regarded as time invariant.

Constant-envelope in cognitive waveform design is discussed to get high power efficiency. Literature [28] presents OFDM optimization waveform design method under the constant-envelope constraint. But constant-envelope condition is too strict in OFDM waveform design. Peak to average power ratio (PAPR) is presented as relaxation form, and the OFDM radar system under the PAPR constraint has been sufficiently studied [12]. If transmitted signal power is very small, the estimation precision may degrade violently and the power spectral density (PSD) of the target TIR cannot be estimated. This is the primary reason why the algorithms in [29] cannot be used directly in CR waveform design. In order to solve this problem, the performance of the TSC estimation should be considered in the CR transmission waveform. A new CR waveform design algorithm for both estimation and detection is studied. In a relative long time, the prior knowledge of the clutter is presented in waveform design [30]. In a pulse duration time, it can be approximately regarded as time invariant in [31]. However, the TIR varies gradually in practice. TSC is varying with the relative motion between the radar and the target. So the TSC estimation update is needed as a feedback.

An iteration approach based on the Kalman filtering (KF) is proposed by Dai et al. in [32] to estimate the TIR for single target. And the transmitted waveform is optimized in order to improve the estimation performances [33]. However, the direct optimization problem of waveform design in the temporal correlated cognitive radar system (CRS) is nonconvex and cannot be solved efficiently. Considering multiple target scenarios, [34, 35] presented a multiple-waveform design algorithm that is based on maximizing a weighted sum of mutual information measures corresponding to the active targets and radar waveforms employed. The related work on designing estimation waveforms for multiple input multiple output (MIMO) radar systems is proposed in [36–38] which discuss the equivalence between maximizing mutual information and minimizing the mean square estimation error (MSE). Therefore, to our best knowledge, only an indirect approach based on the water-filling method is expressed to optimize the PSD of transmitted waveform for single target [13]. No existing work has considered the direct waveform optimization for multiple extended targets in the temporal correlation CRS.

1.2. Contributions. In this paper, we combine the temporal correlated cognitive algorithm presented in [22] and M-ary position phase shift keying (MPPSK) technique [26] to obtain an optimization waveform, which offers superior radar performance and high data rate communication capability between cognitive radar-communication (CRC) transceivers. With this method, the radar and communication signals can coexist by sharing the same frequency band. Hence, the target parameter estimation is not affected by the communication signal design parameters. The UWB-MPPSK waveforms would not only benefit from a KF approach for target estimation and detection but also establish ad hoc communication links. The main contributions of this paper are summarized as follows:

(1) We present a novel MPPSK-based radar-communication waveform design scheme.

(2) We propose a cognitive radar probing strategy based on Kalman filtering between successive backscatter pulses for TSC estimation.

(3) We provide performance analysis of the CRC network in terms of the TSC estimation and communication BER between CRC transceivers.

The organization of this paper is as follows. In Section 2, the CRC transceiver network and the node system architecture are described. In Section 3, we analyze the performance of the communication link achieved through the MPPSK-based waveform. The Kalman filtering-based cognitive waveform optimization approaches are presented in Section 4. The simulation results illustrating the proposed methods are provided in Section 5, and conclusions are given in Section 6.

Throughout this paper, the following notations will be used. Vectors are denoted by boldface lowercase letters and matrices by boldface uppercase letters. H and Re( ) denote transpose conjugate operation and the real part of a variable, respectively. The l_2 norm is denoted as $\| \ \|_2$, linear convolution operator as $*$, expectation operator as $E\{ \}$, and variance operator as Var$\{\cdot\}$.

2. Channel Model

2.1. Target Channel Model. The received echo can be represented as the convolution of the TIR $q(t)$ with the transmission waveform $f(t)$, the additive white Gaussian noise (AWGN) $n(t)$, which can be written as

$$r(t) = q(t) * f(t) + n(t). \tag{1}$$

A model in radar transmission waveform optimization is shown in Figure 1.

During the kth pulse, the TIR between the transmit antennas and the receive antenna is defined as $\mathbf{q}_k$. We denote the cognitive radar waveform that will be emitted from the transmitter as $\mathbf{f}_k \triangleq [f_k(1), f_k(2), \ldots, f_k(N)]^T$, where N is the sample number of cognitive radar waveform. The total transmission energy is $(1/N)\sum_{n=1}^{N} |f_k(n)|^2 = E_f$. $\mathbf{A}$ denotes channel attenuation factor. Let $\mathbf{n} \sim \mathbb{C}N(0, \mathbf{R}_N)$ represent the AWGN. $\mathbf{R}_N$ denotes the covariance matrix of noise. If a target exists, the received scattered signal can be described as

$$\begin{aligned} \mathbf{r}_k &= \mathbf{A}\,\mathrm{diag}\{\mathbf{q}_k\}\,\mathbf{f}_k + \mathbf{n} \\ &= \mathbf{A}\mathbf{Q}_k\mathbf{f}_k + \mathbf{n}. \end{aligned} \tag{2}$$

It is difficult to optimize the transmitted waveform with the convolution operation in the time domain. The complexity of waveform design is increased and cannot be solved efficiently. The echo waveforms in the CRS will be processed in the frequency domain. The received signal vector $\mathbf{y}_k$ can be represented as

$$\mathbf{y}_k \triangleq \Gamma\mathbf{r}_k, \tag{3}$$

where Γ is the matrix of the Fourier transform. The echo waveform in the frequency domain can be described as

$$\mathbf{y}_k = \mathbf{A}\mathbf{Z}_k\mathbf{g}_k + \mathbf{w}. \tag{4}$$

The transmitted waveform is given by a diagonal matrix $\mathbf{Z}_k \triangleq \mathrm{diag}\{\mathbf{z}_k\}$ and the waveform in the frequency domain is $\mathbf{z}_k \triangleq \Gamma\mathbf{f}_k$. $\mathbf{g}_k^T \triangleq \Gamma\mathbf{h}_k^T$ denotes the TSC. $\mathbf{g}_k \sim \mathbb{C}N(0, \mathbf{R}_T)$, $\mathbf{w}_k \sim \mathbb{C}N(0, \mathbf{R}_N)$ denotes AWGN. $\mathbf{R}_T$ and $\mathbf{R}_N$ denote the covariance matrix of target and noise, respectively.

Multiple-pulse samples for the TIR estimation are taken into consideration. From the literature, if these fluctuations are temporally correlated during the pulse repetition interval (PRI), this type of the extended target is closely related to the target radar cross section (RCS) and can be described by a wide sense stationary-uncorrelated scattering (WSSUS) model. The TIR during the kth pulse sample is

$$\mathbf{q}_k = e^{-T/\tau}\mathbf{q}_{k-1} + \mathbf{u}_{k-1}, \tag{5}$$

where $\mathbf{u}_{k-1} \sim \mathbb{N}\{0, (1 - e^{2T/\tau})\mathbf{R}_N\}$ is the zero mean Gaussian vector, k is the index of radar pulses, T denotes the radar pulses interval, and τ describes the temporal correlation of TIR during the pulses interval. The frequency domain characterization of the extended target can be derived by the Wiener-Khintchine theorem [27]. TSC model can be expressed in the frequency domain

$$\mathbf{g}_k = e^{-T/\tau}\mathbf{g}_{k-1} + \mathbf{v}_{k-1}, \tag{6}$$

where $\mathbf{v}_{k-1} \sim \mathbb{N}\{0, (1 - e^{2T/\tau})\mathbf{R}_N\}$ is the zero mean Gaussian vector.

3. Waveform Design

3.1. UWB-MPPSK Waveforms. Each normalized second derivative Gaussian UWB waveform can be represented as

$$\begin{aligned} u(t) = \sum_{i=1}^{I} a_i &\left[1 - 4\pi\left(\frac{t - \alpha_i T}{T_p}\right)^2\right] \\ &\cdot \exp\left\{-2\pi\left(\frac{t - \alpha_i T}{T_P}\right)^2\right\}\cos(\theta_i), \end{aligned} \tag{7}$$

where I is the number of second derivative Gaussian monocycles within the UWB waveform and T_P is the pulse width of the single UWB pulse and is assumed to be 0.2 ns, which is a value commonly used in UWB ranging applications. α_i represents the normalized amplitude of the ith monocycle, which is uniformly distributed, $\alpha_i T$ is the uniformly distributed random pulse repetition time between $[0, T]$, and θ_i represents the phase of the ith pulse. The phase θ_i is chosen as 0 or π in accordance with a pseudorandom binary sequence. MPPSK modulated waveforms are defined as follows:

$$g_0(t) = \sin 2\pi f_c t, \quad 0 \le t < NT_c,$$

$$g_1(t) = \begin{cases} \sin(2\pi f_c t) & 0 \le t \le (k-1)KT_c, \\ -\sin(2\pi f_c t) & (k-1)KT_c < t < kKT_c, \\ \sin(2\pi f_c t) & KT_c \le t < NT_c; \end{cases} \tag{8}$$

$$1 \le k \le M - 1$$

with $g_0(t)$ and $g_1(t)$ being modulation waveforms of symbol "0" and "$m(m > 0)$" and f_c and T_c represent the carrier

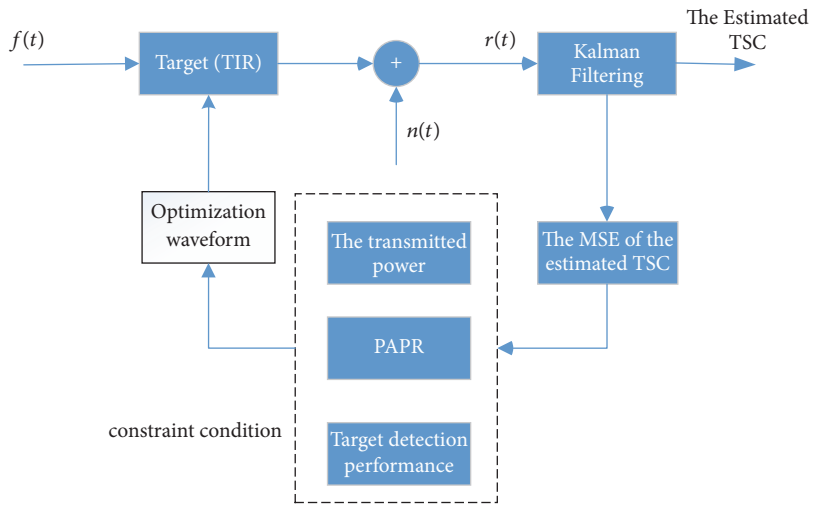

Figure 1: The system model of the temporal correlated cognitive transceiver.

frequency and the carrier period, respectively. K and N stand for the number of the carrier period in each time slot and the number of the carrier period in each symbol, respectively. N/K means the slot number in each symbol, m ($m = 0, 1, \ldots, M-1$) is M-ary ($M \geq 2$) source symbol. Hence, increased M leads to higher data rate as more time slots are utilized. The waveforms of 4-PPSK modulation are illustrated as in Figure 2. The coefficient for the x-axis is the index of a certain sample point. Set $M = 4$; $K = 2$; $N = 20$.

The modulation waveform for symbol "0" is sinusoidal as shown in Figure 2(a); Figure 2(b) illustrates the modulation waveform for symbol "1" with the phase hopping during the first two carrier period (from 0 to 20), the next (from 20 to 40) is for symbol "2" in Figure 2(c), and last (from 40 to 60) is for symbol "3" in Figure 2(d).

The MPPSK modulated signal has the capability of high precise ranging measurement. The time hopping scheme for MPPSK waveform has been analyzed in the literature [39]. The UWB-MPPSK pulse waveforms are defined by

$$\begin{aligned} f_0(t) &= g_0(t)\, u(t), \\ &\qquad 0 \leq t < NT,\ 0 \leq t \leq (m-1)\, KT_c, \\ f_1(t) &= g_1(t)\, u(t), \\ &\qquad (m-1)\, KT_c < t < mKT_c,\ KT_c \leq t < NT_c; \\ &\qquad 1 \leq m \leq M-1 \end{aligned} \tag{9}$$

with $f_0(t)$ and $f_1(t)$ being modulation waveforms of symbols "0" and "1." UWB-MPPSK waveform communications offer high data rates for communications and good immunity against multipath fading over short ranges. According to the literature [39], the BER for such a UWB-MPPSK waveform is given as

$$P_e = \frac{1}{2}\left[1 + Q_1\left(\frac{A_0}{\delta}, \frac{u_T}{\delta}\right) - Q_2\left(\frac{(1+k)\, A_0}{\delta}, \frac{u_T}{\delta}\right)\right], \tag{10}$$

where A_0 denotes the amplitude of transmitted signal. $Q_1(a, b)$ is Marcum's function, which can be defined as follows:

$$Q_1(a, b) = e^{-(a^2+b^2)/2} \sum_{k=0}^{\infty} \left(\frac{a}{b}\right)^k I_k(ab). \tag{11}$$

3.2. System Architecture and CRC Waveform Design. We design the CRC waveforms by introducing UWB-MPPSK waveform for communication and radar functionalities in this paper. The proposed phase-coded waveform is transmitted to detect target and send the data to other receivers. The received signal includes the radar echoes reflected from target and the communication information from other receivers. The received signal is passed on to a matched filter bank. Communication data is extracted by MPPSK demodulation. And the radar echo is sent to the target parameter estimation for target detection. The system architecture of the CRC transceiver is described in Figure 3.

UWB-MPPSK waveform design feedback loop is shown in Figure 4.

The waveform ensemble consists of individual MPPSK-based UWB waveforms in which the PRI, amplitude, and phase are dictated by uniformly distributed random variables. It is also assumed that the receiver has full knowledge of the transmitted waveform. A generalized likelihood ratio test (GLRT) is adopted to detect the presence of the target in a particular range-Doppler bin. The TSC estimation in the frequency domain based on the KF is proposed to exploit this temporal correlation at the receiver. The waveform optimization is modeled to minimize the MSE at the transmitter.

The proposed cognitive waveform design feedback loop is summarized as follows:

(1) The CRC transceiver updates TSC by successive measurements of the radar scene.

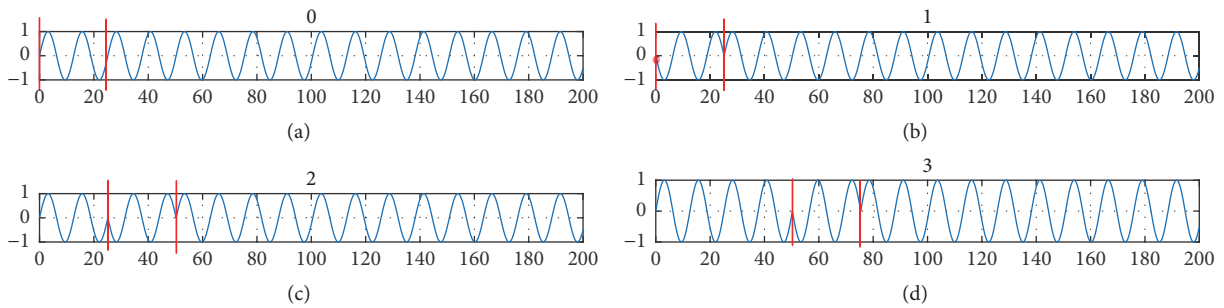

Figure 2: 4PPSK modulated waveforms.

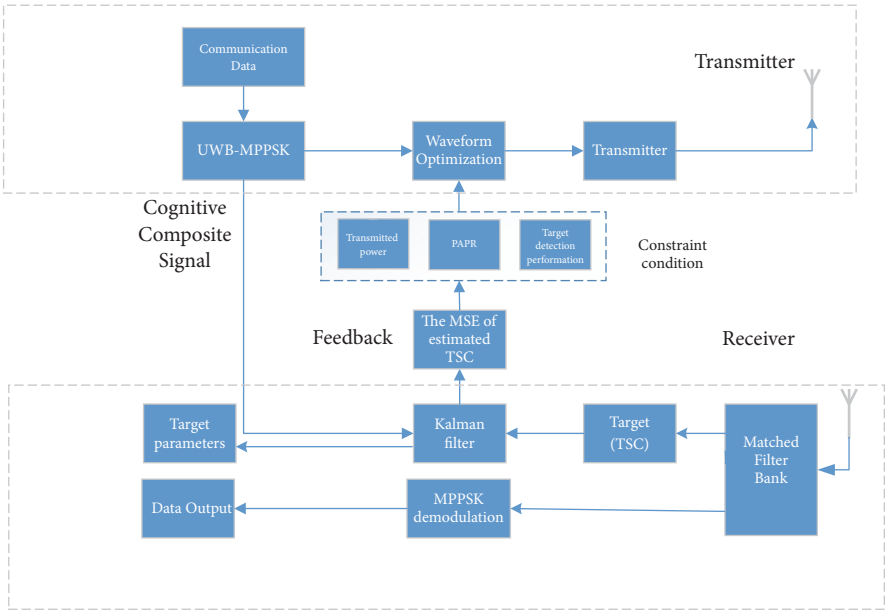

Figure 3: The system architecture of the CRC transceiver.

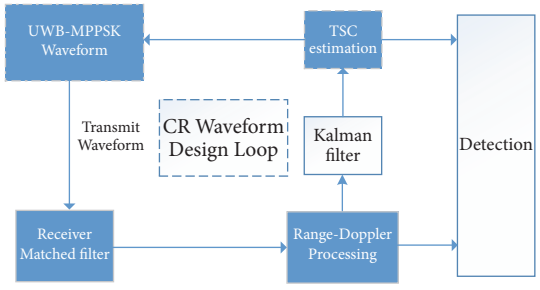

Figure 4: Cognitive waveform design feedback loop.

(2) The CRC transceiver adapts its UWB-MPPSK waveform and selects a suitable UWB-MPPSK waveform in the next time instant.

(3) The cognitive waveform design feedback loop from the receiver to the transmitter allows the delivery of TSC to the transmitter. Transmitter utilizes the TSC to select the optimal waveform based on Kalman filtering for transmission.

(4) The process is repeated iteratively.

4. KF-Based Waveform Optimization

4.1. TSC Estimation Based on MAP Criterion. In the wideband cognitive radar system, the extended target has a complex target impulse response (TIR), which is the target scattering coefficient (TSC) in the frequency domain. Reference [13, 14] model the extended target as a wide sense stationary-uncorrelated scattering TIR model, considering the change of target view angle and the strong correlation of TSC during the pluses interval. The target scattering is modeled as a linear system. By the Bayesian rule, the TSC estimation algorithm based on maximum a posteriori (MAP) in AWGN channel can be written as

$$\hat{\mathbf{g}}_k = \arg\max_{\mathbf{g}_k} p\left(\mathbf{g}_k \mid \mathbf{y}_k\right) = \arg\max_{\mathbf{g}_k} \frac{p\left(\mathbf{y}_k \mid \mathbf{g}_k\right) p\left(\mathbf{g}_k\right)}{p\left(\mathbf{y}_k\right)}, \quad (12)$$

where

$$p(\mathbf{y}_k \mid \mathbf{g}_k) = \frac{1}{(2\pi)^{M/2}\left|\mathbf{R}_N\right|^{1/2}} \cdot \exp\left(-\frac{1}{2}(\mathbf{y}_k - \mathbf{A}_k\mathbf{Z}_k\mathbf{g}_k)^H \mathbf{R}_N^{-1}(\mathbf{y}_k - \mathbf{A}_k\mathbf{Z}_k\mathbf{g}_k)\right),$$

$$p(\mathbf{g}_k) = \frac{1}{(2\pi)^{M/2}\left|\mathbf{R}_T\right|^{1/2}} \exp\left(-\frac{1}{2}(\mathbf{g}_k)^H \mathbf{R}_T^{-1}\mathbf{g}_k\right),$$
$$p(\mathbf{y}_k) = \int p(\mathbf{y}_k \mid \mathbf{g}_k)\, p(\mathbf{g}_k)\, d\mathbf{g}_k. \tag{13}$$

We can obtain the posterior probability

$$p(\mathbf{g}_k \mid \mathbf{y}_k) = \frac{p(\mathbf{y}_k \mid \mathbf{g}_k)\, p(\mathbf{g}_k)}{p(\mathbf{y}_k)} = \frac{\exp\left(\left(1/\sigma_n^2\right)(\mathbf{A}_k\mathbf{Z}_k\mathbf{g}_k)^T \mathbf{y}_k - \left(1/2\sigma_n^2\right)(\mathbf{A}_k\mathbf{Z}_k\mathbf{g}_k)^T \mathbf{A}_k\mathbf{Z}_k\mathbf{g}_k - (1/2)(\mathbf{g}_k)^T \mathbf{R}_T^{-1}(\mathbf{g}_k)\right)}{\exp\left((1/2)\left((\mathbf{A}_k\mathbf{Z}_k)^T \mathbf{y}_k/\sigma_n^2\right)^T \left((1/\sigma_n^2)(\mathbf{A}_k\mathbf{Z}_k)^T \mathbf{A}_k\mathbf{Z}_k + \mathbf{R}_T^{-1}\right)^{-T}\left((\mathbf{A}_k\mathbf{Z}_k)^T \mathbf{y}_k/\sigma_n^2\right)\right)\sqrt{\left|2\pi\left((1/\sigma_n^2)(\mathbf{A}_k\mathbf{Z}_k)^T \mathbf{A}_k\mathbf{Z}_k + \mathbf{R}_T^{-1}\right)^{-1}\right|}}. \tag{14}$$

The received waveform $\mathbf{y}_k$ follows Gaussian distribution given $\mathbf{y}_k \mid \mathbf{g}_k \sim \mathbb{C}N(\mathbf{A}_k\mathbf{Z}_k\mathbf{g}_k, \mathbf{R}_N)$ and $p(\mathbf{g}_k \mid \mathbf{y}_k)$ is the probability distribution of TSC during the kth pulse. So the estimation of TSC in the frequency domain with MAP estimation is

$$\widehat{\mathbf{g}}_k = \underset{\mathbf{g}_k}{\operatorname{argmax}}\left\{-\frac{1}{2}\mathbf{g}_k^T\left(\frac{1}{\sigma_n^2}(\mathbf{A}_k\mathbf{Z}_k)^T \mathbf{A}_k\mathbf{Z}_k + \mathbf{R}_N^{-1}\right)\mathbf{g}_k + \frac{1}{\sigma_n^2}(\mathbf{A}_k\mathbf{Z}_k\mathbf{g}_k)^T \mathbf{y}_k\right\} = \left((\mathbf{A}_k\mathbf{Z}_k)^T \mathbf{A}_k\mathbf{Z}_k + \sigma_n^2\mathbf{R}_N^{-1}\right)^{-1}(\mathbf{A}_k\mathbf{Z}_k)^T \mathbf{y}_k. \tag{15}$$

The receiver filter can be denoted as the matrix form $\mathbf{Q}_k$:

$$\mathbf{Q}_k = \left((\mathbf{A}_k\mathbf{Z}_k)^T \mathbf{A}_k\mathbf{Z}_k + \sigma_n^2\mathbf{R}_N^{-1}\right)^{-1}(\mathbf{A}_k\mathbf{Z}_k)^T. \tag{16}$$

We have $\widehat{\mathbf{g}}_k = \mathbf{Q}_k\mathbf{y}_k$. Now let the transmitted waveforms be $\mathbf{S}_k = \mathbf{A}_k\mathbf{Z}_k$. Thus, the mean square error (MSE) of MAP estimation can be obtained by

$$e_k = E\left\{\left\|\widehat{\mathbf{g}}_k - \mathbf{g}_k\right\|_2^2\right\} = \mathscr{E}\left\{(\mathbf{Q}_k\mathbf{y}_k - \mathbf{g}_k)(\mathbf{Q}_k\mathbf{y}_k - \mathbf{g}_k)^H\right\} = \mathbf{Q}_k\left(\mathbf{S}_k\mathbf{R}_T\mathbf{S}_k^H + \mathbf{R}_N\right)\mathbf{Q}_k^H - \mathbf{Q}_k\mathbf{S}_k\mathbf{R}_T - \mathbf{R}_T\mathbf{S}_k^H\mathbf{Q}_k^H + \mathbf{R}_T. \tag{17}$$

4.2. Waveform Optimization. Since the time correlation of the TSC, a KF-based estimation method is proposed to estimate TSC when the GLRT detection shows the presence of target in this paper. The TSC estimation performance can be improved by taking the advantage of prediction and estimation at the same time. The iteration process is described in Appendix (Algorithm 1).

Considering transmitted power E_f, PAPR σ, and target detection probability ε constraints, the multiple-pulse samples of wideband radar waveform based on Kalman filtering are designed by minimizing the MSE of estimation TSC. The optimization waveform design problem can be preliminary described as follows:

$$\begin{aligned}
&\mathbf{f} = \arg\min_{\mathbf{f}}\left\{\operatorname{tr}\left(\mathbf{P}_{k|k}\right)\right\}\\
&\text{s.t.}\quad \sum_{k=1}^{K} P_q(\omega_k)\, P_f(\omega_k) - \sum_{k=1}^{K} P_n(\omega_k) \geq 0\\
&\mathbf{f}^H\mathbf{f} \leq E_f\\
&\text{PAPR} \leq \zeta\\
&P_D \geq \varepsilon.
\end{aligned} \tag{18}$$

The objective function is the MSE of estimation TSC based on Kalman filtering, which can be simplified as follows:

$$\mathbf{P}_{k|k} = \left(\left(\mathbf{P}_{k|k-1}\right)^{-1} + (\mathbf{Q}_k\mathbf{A}_k\mathbf{Z}_k)^H\left(\mathbf{Q}_k\mathbf{R}_N(\mathbf{Q}_k)^H\right)^{-1}\mathbf{Q}_k\mathbf{A}_k\mathbf{Z}_k\right)^{-1} = \left(\left(\mathbf{P}_{k|k-1}\right)^{-1} + (\mathbf{A}_k\mathbf{Z}_k)^H(\mathbf{R}_N)^{-1}\mathbf{A}_k\mathbf{Z}_k\right)^{-1}. \tag{19}$$

From literature (18), (19) can be rewritten as

$$\begin{aligned}
&\mathbf{z} = \arg\min_{\mathbf{z}}\left\{\operatorname{tr}\left(\left(\left(\mathbf{P}_{k|k-1}\right)^{-1} + (\mathbf{A}_k\mathbf{Z}_k)^H\mathbf{R}_N^{-1}\mathbf{A}_k\mathbf{Z}_k\right)^{-1}\right)\right\}\\
&\text{s.t.}\quad \sum_{k=1}^{K} P_q(\omega_k)\, P_f(\omega_k) - \sum_{k=1}^{K} P_n(\omega_k) \geq 0\\
&\mathbf{z}^H\mathbf{z} \leq E_f\\
&\sqrt{\sigma E_f}\mathbf{I} - \operatorname{diag}\{\mathbf{f}\} \geq 0\\
&\sqrt{\sigma E_f}\mathbf{I} + \operatorname{diag}\{\mathbf{f}\} \geq 0\\
&\mathbf{z}^H\widehat{\mathbf{Q}}_k{}^H\mathbf{R}_N^{-1}\widehat{\mathbf{Q}}_k\mathbf{z} \geq \varepsilon'.
\end{aligned} \tag{20}$$

The fixed value is obtained if $\widehat{\mathbf{z}}$ is the eigenvector of $\widehat{\mathbf{Q}}_k{}^H\mathbf{R}_N^{-1}\widehat{\mathbf{Q}}_k$ with the maximum eigenvalue [28]. Then we have $\max p(\mathbf{z}) = \lambda_{\max}E_f$. $\lambda_{\max}$ is the maximum eigenvalue of $\widehat{\mathbf{Q}}_k{}^H\mathbf{R}_N^{-1}\widehat{\mathbf{Q}}_k$.

Step 1. Set iteration index as $k = 1$, and the initial MSE matrix of estimation TSC

Step 2. Utilizing the temporal correlation of TSC, we can get the prediction of TSC

$$\widehat{\mathbf{g}}_{k|k-1} = e^{-T/\tau}\widehat{\mathbf{g}}_{k-1|k-1}$$

Step 3. According to the prediction of TSC, the estimation MSE matrix is

$$\mathbf{P}_{k|k-1} = e^{-2T/\tau}\mathbf{P}_{k-1|k-1} + (1 - e^{-2T/\tau})\mathbf{R}_T$$

Step 4. Define the Kalman gain matrix as

$$\mathbf{\Phi}_k = \mathbf{P}_{k|k-1}(\mathbf{Q}_k\mathbf{A}_k\mathbf{Z}_k)^H[(\mathbf{Q}_k\mathbf{A}_k\mathbf{Z}_k)\mathbf{P}_{k|k-1}(\mathbf{Q}_k\mathbf{A}_k\mathbf{Z}_k)^H + \mathbf{Q}_k\mathbf{R}_N(\mathbf{Q}_k)^H]^{-1}$$

Step 5. The estimation of TSC is

$$\widehat{\mathbf{g}}_{k|k} = \widehat{\mathbf{g}}_{k|k-1} + \mathbf{\Phi}_k(\widehat{\mathbf{g}}_k - \mathbf{Q}_k\mathbf{A}_k\mathbf{Z}_k\widehat{\mathbf{g}}_{k|k-1})$$

$$\widehat{\mathbf{g}}_k = \mathbf{Q}_k\mathbf{y}_k$$

where $\widehat{\mathbf{g}}_k$ is the estimated values based on the MAP estimation

Step 6. The MSE matrix is

$$\mathbf{P}_{k|k} = \mathbf{P}_{k|k-1} - \mathbf{\Phi}_k\mathbf{Q}_k\mathbf{A}_k\mathbf{Z}_k\mathbf{P}_{k|k-1}$$

If $k = K_{\max}$ end; Otherwise, iterate Step 2 to Step 6.

Algorithm 1: Kalman filtering for TSC estimation in CRC system.

This optimization problem is convex satisfying the condition $\lambda_{\max}E_f \geq \varepsilon'$. If $\text{rank}(\mathbf{f}\mathbf{f}^H) = 1$, $\mathbf{f}_0$ is the optimal radar waveform. According to [30], the optimal signal waveform with $\text{rank}(\mathbf{f}\mathbf{f}^H) > 1$ can be obtained via CVX toolbox. In each iteration, determining whether the feasible set is empty can be evaluated by solving a feasibility problem using the CVX toolbox.

The MPPSK modulated CR waveform design algorithm can be summarized as follows:

(1) The MPPSK modulated CR waveform embedded the communication data is transmitted.

(2) The radar echoes $\mathbf{y}_k$ are used to estimate the MSE matrix of the TSC $\mathbf{P}_{k|k}$, which are updated using the current radar echoes and are relayed back to the Kalman filtering.

(3) The received communication signals are passed through a matched filter bank, which demodulates MPPSK modulated waveform.

5. Simulation Results and Discussion

Firstly, we set the MPPSK modulation parameter $M \leq 3$; $N = 10$; $K = 5$ make sure that the cross-correlation coefficient between the transmission waveforms $\Delta \leq 0.4$. In this way, we can obtain an acceptable BER for communications [39]. As described in the previous sections, the orthogonality between CRC transmission waveforms is maintained for radar waveform optimization purposes.

Next, the received signal is matched filtered to estimate the propagation delay. The communication data are demodulated and the radar signal processing is carried out by the TSC estimation module, separately. The MSE matrix of the TSC is estimated by using Kalman filtering in the subsequent time interval. We use the normalized MSE to defining the estimation performance.

$$n\text{MSE} = \frac{\|\widehat{\mathbf{g}} - \mathbf{g}\|_2^2}{\|\mathbf{g}\|_2^2}, \tag{21}$$

Table 1: Simulation parameters 2.

E_s	Transmitted power	1
ASNR	Average signal noise ratio	8 dB
τ	Temporal correlation	0.1 s
M_t	Pulse interval	1 ms
p_{fa}	False alarm probability	0.05
p_d	Detection probability	0.95
PAPR	Peak to average power ratio	3 dB
f_s	The sampling frequency	10 GHz
f_c	Center frequency of UWB	3 GHz

where $\widehat{\mathbf{g}}$ and $\mathbf{g}$ denote the estimation TSC and the real measurement data, respectively. The simulation parameters are shown in Table 1.

Figure 5 shows the detection probability based on the Neyman-Pearson criterion for false alarm probability $p_{\text{fa}} = 5\%$. For a stationary radar scene, 800 simulations have been run for each SNR. The next CRC waveform is chosen according to the Kalman filtering algorithm, and the process is repeated for 20 iterations. As seen from Figure 4, the proposed algorithm converges after 10 iterations, yielding a detection probability of 0.9 at SNR = 6 dB as compared to SNR = 15 dB at the first iteration. However, the detection probability does not show further improvement after 15 iterations.

In Figure 6, we compare the detection probability for optimization waveforms selected by the proposed algorithm to the probability for waveform based on MI minimization and compare this result with the random waveform in multipath environments. As the proposed algorithm utilizes the temporal correlation of TIR during the pulses interval, the CRC transceiver adapts its radar signal better than waveform based MI minimization to the fluctuating target RCS. On the other hand, random waveform is unable to match the time-varying TSC after multiple iterations. Hence, the detection probability is suboptimal in this case.

In Figure 7, under the constraint of transmitted power and ASNR, we compare the TSC estimation performance

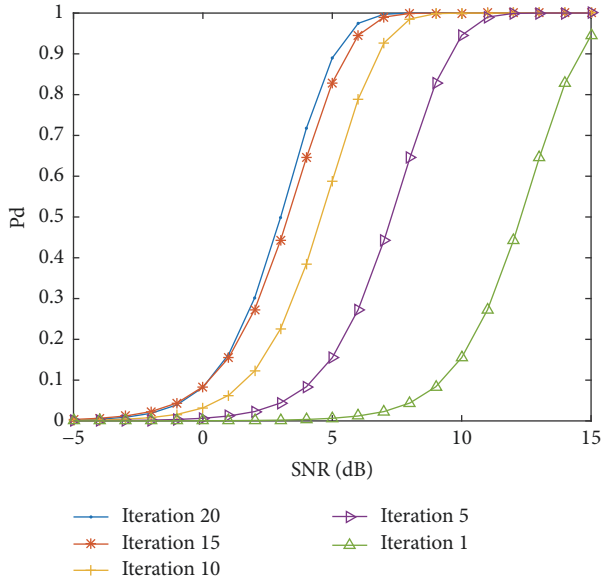

Figure 5: Detection probability for various iterations of the Kalman filtering approach.

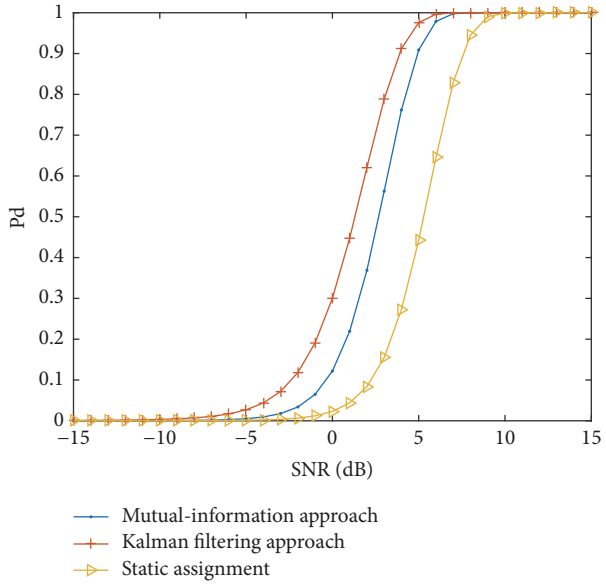

Figure 6: Detection probability for optimization waveforms based on Kalman filtering approach and random waveform.

based on the Kalman filtering algorithm and MAP estimation criterion in multipath environments. As seen from Figure 7, the normalized MSE of TSC estimation based on the Kalman filtering algorithm is smaller than that using the MAP criterion. Similarly, the normalized MSE of TSC estimation regarding clutter based on Kalman filtering is smaller than that regardless clutter. In Figure 8, under the constraints of transmitted power, PAPR, ASNR, and detection probability, we also compare the normalized MSE of TSC estimation based on the Kalman filtering algorithm and MAP estimation criterion. The TSC estimation performances of optimization

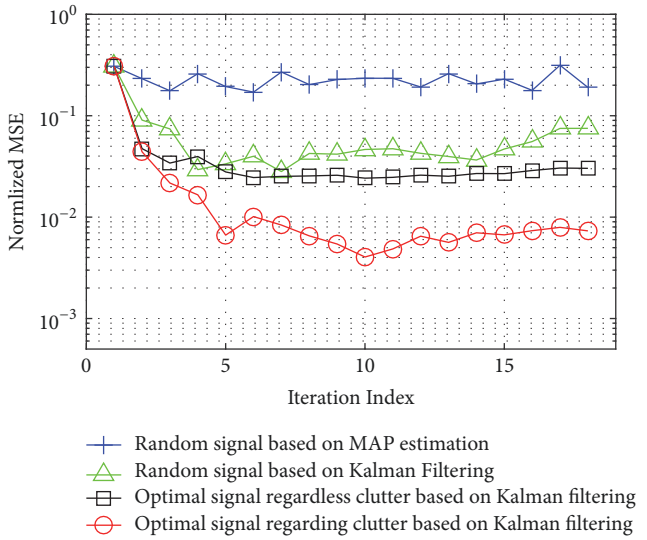

Figure 7: The MSE of TSC estimation under power and SNR.

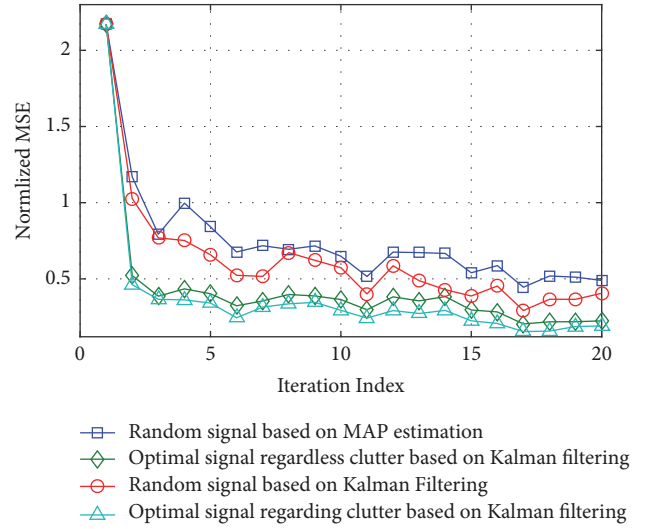

Figure 8: The MSE of TSC estimation under power, SNR, PAPR, and detection constraint.

waveform and random waveform are compared, to verify the efficiency of optimizing waveform at each Kalman filtering iteration step.

We discuss the performance of the UWB-MPPSK waveform from a communications perspective in this subsection. Figure 9 illustrates the BER for the UWB-MPPSK waveforms and UWB-OFDM waveforms.

As seen from Figure 9, the SNR performance of Binary UWB-MPPSK signal may be improved by approximately 1 dB, 4 dB, and 8 dB as compared with Binary UWB-PPM, 4-ary UWB-MPPSK, and 16-ary UWB-MPPSK, respectively. OFDM signals offer better bit error performance. However, the MPPSK design performs comparably to OFDM schemes when no data redundancy bit for error control is added.

From (9), the data rate of MPPSK signal is proportional to carrier frequency and modulation parameter M, but inversely

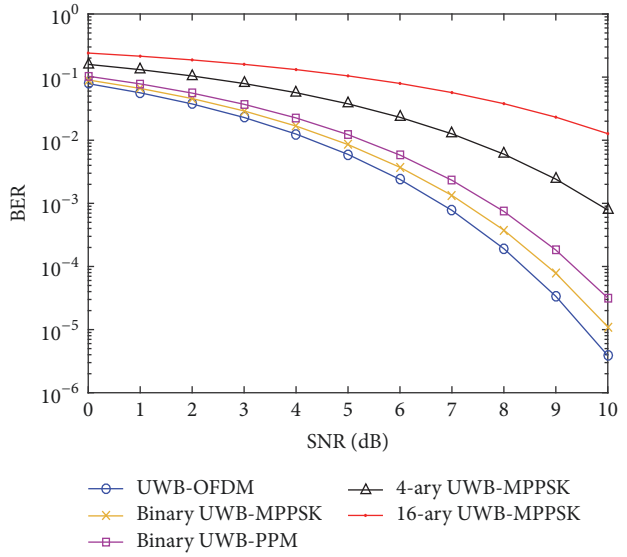

Figure 9: Comparative SER results of UWB-OFDM, Binary UWB-MPPSK, 4-ary UWB-MPPSK, and 16-ary UWB-MPPSK.

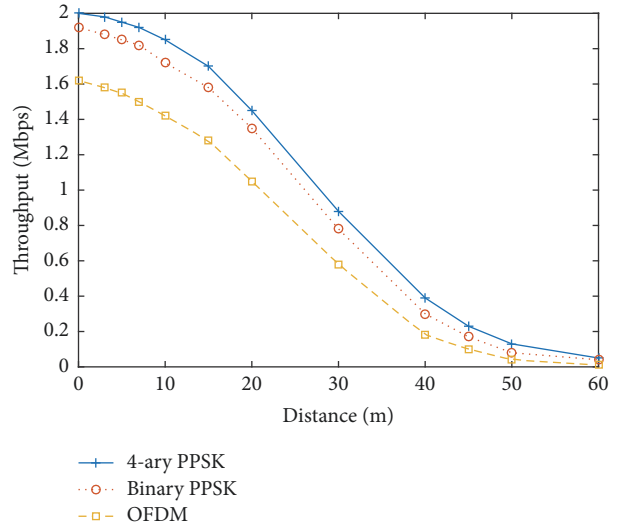

Figure 10: Comparative throughput performance of UWB-OFDM, Binary UWB-MPPSK, and 4-ary UWB-MPPSK.

proportional to modulation parameter N. Setting modulation parameter $N = 10; M = 4$, down-conversion IF = 100 MHz, and duty cycle of the pulse signal $T = 1/10$, pulse width is $\tau = 20\,\mu$s. We can obtain burst transmission data rate $2 * 100/10 * 1/10 = 2$ Mbps.

Figure 10 presents the throughput result for the proposed waveform as compared to OFDM waveform. 4-ary PPSK waveform offers a burst transmission data rate of about 1.8 Mbps at a distance of 15 m, which is better than that offered by the four-carrier OFDM. UWB communications achieve high data rate over short distances, as the distance between the transceivers increases the throughput falls. According to the relational expression:

$$\begin{aligned}&\text{Data volume of a beam}\\&= \text{Bit rate} \times \text{Pulse width} \times \text{Pulse number}.\end{aligned} \tag{22}$$

Since the MPPSK-based CRC transceiver transmits 20 pulses within a radar beam, we can obtain burst transmission data volume $20 * 4000/10 = 8$ kB. However, as modulation parameter M is increased, the sidelobes in the autocorrelation plot become more prominent. This distorts the orthogonality of the MPPSK waveform and in turn may deteriorate the target detection performance. So we choose reasonable MPPSK modulation parameters results in a tradeoff between communication and radar signal design requirements.

6. Conclusion

In this paper, a waveform design concept for a CRC transceiver system has been studied that allow for simultaneous wireless communications and radar operation. A new UWB-MPPSK modulation scheme is proposed for integrated waveform design. The Kalman filtering-based waveform optimization approach is addressed for improving the target estimation performance. The proposed approach is based upon learning about the detection environment and adjusting the transmission waveform characteristics to suit the dynamic target scene. The implementation has been shown to offer many advantages regarding the performance of the radar application, in particular, better TSC estimation performance and independence from the transmitted user data. The proposed method also facilitates high data rate performance for the communications application. The discussed waveform design concepts offer interesting perspectives for the realization of future sensor devices in intelligent transportation system.

Appendix

Kalman Filtering for TSC Estimation in CRC System

The KF-based TSC estimation in the frequency domain has been discussed. The estimation performance is improved by exploiting the temporal correlation of TSC. Compared with the convolution operation in the time domain, the complexity of waveform design for TSC estimation in the frequency is reduced (see Algorithm 1).

Conflicts of Interest

The authors declare no conflicts of interest.

Acknowledgments

This work was supported by the National Natural Science Foundation of China (61761019).

References

[1] D. W. Bliss, "Cooperative radar and communications signaling: the estimation and information theory odd couple," in *Proceedings of the 2014 IEEE Radar Conference, RadarCon 2014*, pp. 50–55, Cincinnatim, Ohio, USA, 2014.

[2] J. R. Guerci, R. M. Guerci, A. Lackpour, and D. Moskowitz, "Joint design and operation of shared spectrum access for radar and communications," in *Proceedings of the 2015 IEEE International Radar Conference, RadarCon 2015*, pp. 761–766, USA, May 2015.

[3] A. R. Chiriyath, B. Paul, G. M. Jacyna, and D. W. Bliss, "Inner bounds on performance of radar and communications coexistence," *IEEE Transactions on Signal Processing*, vol. 64, no. 2, pp. 464–474, 2016.

[4] A. R. Chiriyath, B. Paul, and D. W. Bliss, "Joint radar-communications information bounds with clutter: The phase noise menace," in *Proceedings of the 2016 IEEE Radar Conference, RadarConf 2016*, USA, May 2016.

[5] J. S. Kwak and J. H. Lee, "Infrared Transmission for Intervehicle Ranging and Vehicle-to-roadside Communication Systems Using Spread-Spectrum Technique," *IEEE Transactions on Intelligent Transportation Systems*, vol. 5, no. 1, pp. 12–19, 2004.

[6] A. Hassanien, M. G. Amin, Y. D. Zhang, and F. Ahmad, "Dual-function radar-communications: information embedding using sidelobe control and waveform diversity," *IEEE Transactions on Signal Processing*, vol. 64, no. 8, pp. 2168–2181, 2016.

[7] L. Han and K. Wu, "24-GHz integrated radio and radar system capable of time-agile wireless communication and sensing," *IEEE Transactions on Microwave Theory and Techniques*, vol. 60, no. 3, pp. 619–631, 2012.

[8] A. Sabharwal, P. Schniter, D. Guo, D. W. Bliss, S. Rangarajan, and R. Wichman, "In-band full-duplex wireless: challenges and opportunities," *IEEE Journal on Selected Areas in Communications*, vol. 32, no. 9, pp. 1637–1652, 2014.

[9] H. Takase and M. Shinriki, "A dual-use radar and communication system with complete complementary codes," in *Proceedings of the 2014 15th International Radar Symposium, IRS 2014*, Poland, June 2014.

[10] D. Ciuonzo, A. De Maio, G. Foglia, and M. Piezzo, "Intrapulse radar-embedded communications via multiobjective optimization," *IEEE Transactions on Aerospace and Electronic Systems*, vol. 51, no. 4, pp. 2960–2974, 2015.

[11] Y. L. Sit and T. Zwick, "MIMO OFDM radar with communication and interference cancellation features," in *Proceedings of the 2014 IEEE Radar Conference, RadarCon 2014*, pp. 265–268, USA, May 2014.

[12] C. Sturm, T. Zwick, and W. Wiesbeck, "An OFDM system concept for joint radar and communications operations," in *Proceedings of the VTC Spring 2009 - IEEE 69th Vehicular Technology Conference*, 2009.

[13] S. Sen, "PAPR-constrained pareto-optimal waveform design for OFDM-STAP Radar," *IEEE Transactions on Geoscience and Remote Sensing*, vol. 52, no. 6, pp. 3658–3669, 2014.

[14] A. Cailean, B. Cagneau, L. Chassagne, S. Topsu, Y. Alayli, and J.-M. Blosseville, "Visible light communications: Application to cooperation between vehicles and road infrastructures," in *Proceedings of the 2012 IEEE Intelligent Vehicles Symposium, IV 2012*, pp. 1055–1059, Spain, June 2012.

[15] Y. Nijsure, Y. Chen, S. Boussakta, C. Yuen, Y. H. Chew, and Z. Ding, "Novel system architecture and waveform design for cognitive radar radio networks," *IEEE Transactions on Vehicular Technology*, vol. 61, no. 8, pp. 3630–3642, 2012.

[16] Y.-S. Shen, F.-B. Ueng, J.-D. Chen, and S.-T. Huang, "A performance analysis of the high-capacity TH multiple access UWB system using PPM," in *Proceedings of the 2009 IEEE 20th Personal, Indoor and Mobile Radio Communications Symposium, PIMRC 2009*, Japan, September 2009.

[17] N. V. Kokkalis, P. T. Mathiopoulos, G. K. Karagiannidis, and C. S. Koukourlis, "Performance analysis of M-ary PPM TH-UWB systems in the presence of MUI and timing jitter," *IEEE Journal on Selected Areas in Communications*, vol. 24, no. 4 I, pp. 822–828, 2006.

[18] X. Gong, H. Meng, Y. Wei, and X. Wang, "Phase-modulated waveform design for extended target detection in the presence of clutter," *Sensors*, vol. 11, no. 7, pp. 7162–7177, 2011.

[19] S. Haykin, "Cognitive radar," *IEEE Signal Processing Magazine*, vol. 23, no. 1, pp. 30–40, 2006.

[20] Y. Chen and P. Rapajic, "Ultra-wideband cognitive interrogator network: Adaptive illumination with active sensors for target localisation," *IET Communications*, vol. 4, no. 5, pp. 573–584, 2010.

[21] X. Deng, C. Qiu, Z. Cao, M. Morelande, and B. Moran, "Waveform design for enhanced detection of extended target in signal-dependent interference," *IET Radar, Sonar & Navigation*, vol. 6, no. 1, pp. 30–38, 2012.

[22] P. Chen and L. Wu, "Waveform design for multiple extended targets in temporally correlated cognitive radar system," *IET Radar, Sonar & Navigation*, vol. 10, no. 2, pp. 398–410, 2016.

[23] S. Sen and C. W. Glover, "Optimal multicarrier phase-coded waveform design for detection of extended targets," in *Proceedings of the IEEE Radar Conference*, pp. 1–6, Ottawa, Canada, April-May 2013.

[24] X. Zhang and C. Cui, "Range-spread target detecting for cognitive radar based on track-before-detect," *International Journal of Electronics*, vol. 101, no. 1, pp. 74–87, 2014.

[25] L. K. Patton, S. W. Frost, and B. D. Rigling, "Efficient design of radar waveforms for optimised detection in coloured noise," *IET Radar, Sonar & Navigation*, vol. 6, no. 1, pp. 21–29, 2012.

[26] S. Sen, "Characterizations of PAPR-constrained radar waveforms for optimal target detection," *IEEE Sensors Journal*, vol. 14, no. 5, pp. 1647–1654, 2014.

[27] R. A. Romero and N. A. Goodman, "Waveform design in signal-dependent interference and application to target recognition with multiple transmissions," *IET Radar, Sonar & Navigation*, vol. 3, no. 4, pp. 328–340, 2009.

[28] S. C. Thompson and J. P. Stralka, "Constant envelope OFDM for power-efficient radar and data communications," in *Proceedings of the 2009 International Waveform Diversity and Design Conference, WDD 2009*, pp. 291–295, USA, February 2009.

[29] Y. Nijsure, Y. Chen, P. Rapajic, C. Yuen, Y. H. Chew, and T. F. Qin, "Information-theoretic algorithm for waveform optimization within ultra wideband cognitive radar network," in *Proceedings of the 2010 IEEE International Conference on Ultra-Wideband, ICUWB2010*, pp. 595–598, China, September 2010.

[30] N. A. Goodman, P. R. Venkata, and M. A. Neifeld, "Adaptive waveform design and sequential hypothesis testing for target recognition with active sensors," *IEEE Journal of Selected Topics in Signal Processing*, vol. 1, no. 1, pp. 105–113, 2007.

[31] M. Fan, D. Liao, X. Ding, and X. Li, "Waveform design for target recognition on the background of clutter," in *Proceedings of the 8th European Radar Conference, EuRAD 2011, Held as Part of the*

14th European Microwave Week 2011, EuMW 2011, pp. 329–332, gbr, October 2011.

[32] F. Z. Dai, H. W. Liu, P. H. Wang, and S. Z. Xia, "Adaptive waveform design for range-spread target tracking," *IEEE Electronics Letters*, vol. 46, no. 11, pp. 793-794, 2010.

[33] B. Jiu, H. Liu, L. Zhang, Y. Wang, and T. Luo, "Wideband cognitive radar waveform optimization for joint target radar signature estimation and target detection," *IEEE Transactions on Aerospace and Electronic Systems*, vol. 51, no. 2, pp. 1530–1546, 2015.

[34] A. Leshem, O. Naparstek, and A. Nehorai, "Information theoretic adaptive radar waveform design for multiple extended targets," *IEEE Journal of Selected Topics in Signal Processing*, vol. 1, no. 1, pp. 42–55, 2007.

[35] X. Zhang, C. Cui, and J. Yu, "Multiple extended targets tracking for cognitive radar in the presence of signal-dependent clutter," *Journal of Circuits and Systems*, vol. 18, no. 2, pp. 492–499, 2013.

[36] S. Sen and A. Nehorai, "OFDM-MIMO Radar With Mutual-Information Waveform Design for Low-Grazing Angle Tracking," *IEEE Transactions on Signal Processing*, vol. 58, no. 6, pp. 3152–3162, 2010.

[37] T. Huang and T. Zhao, "Low PMEPR OFDM radar waveform design using the iterative least squares algorithm," *IEEE Signal Processing Letters*, vol. 22, no. 11, pp. 1975–1979, 2015.

[38] B. Li and A. Petropulu, "MIMO radar and communication spectrum sharing with clutter mitigation," in *Proceedings of the 2016 IEEE Radar Conference, RadarConf 2016*, USA, May 2016.

[39] C. Lu, L. Wu, P. Chen, J. Wang, and H. Liu, "M-ary phase position shift keying with orthogonal signalling," *IET Communications*, vol. 9, no. 13, pp. 1627–1634, 2015.